Theory Development of Far-field Leakage Magnetic Field in Dynamic Wireless Power Transfer for Electric Vehicles Charging and Influence of Ferrite

Soma HASEGAWA† Takehiro IMURA‡ and Yoichi HORI‡

†Faculty of Science and Technology, Tokyo University of Science 2641 Yamazaki, Noda-shi, Chiba, 278-8510 Japan

Abstract One of the issues of dynamic wireless power transfer for electric vehicles charging is the effect of leakage magnetic fields. In this paper, the far-field leakage magnetic field generated by wireless power transfer is calculated using vector potentials, and the effect of ferrite on the theoretical calculations is examined. Comparison with the results of electromagnetic field analysis using the moment method revealed that the far-field leakage magnetic field can be calculated using the same equation as for an air-core coil, even for a coil with a ferrite core, if the current value flowing through the core is known.

Keyword Dynamic Power Transfer, Wireless Power Transfer, Vector Potentials, Leakage Magnetic Field, EMF

1. INTRODUCTION

Electric vehicles (EV) are attracting attention as a solution to the problems of global warming and dependence on fossil fuels, but they are not widely used. Dynamic Wireless Power Transfer (DWPT) is expected to minimize the capacity of batteries installed in EVs and eliminate limitations on EV range. However, there are various challenges to the practical application of DWPT, one of which is the problem of leakage magnetic field. Leakage magnetic field of WPT for EV is regulated by CISPR and ICNIRP [1], and technology to suppress it is essential. In the EMF problem of EVs, the magnetic field at 1 to 2 m from the coil (near leakage magnetic field) has been actively studied [2][3], but the magnetic field at 10 m away from the coil (far leakage magnetic field) has hardly been studied.

Ferrite is an electronic component material with excellent magnetic properties. The high permeability and low loss tangent are expected to improve WPT performance, and many studies have been conducted on its application to WPT for EVs [4]. Furthermore, ferrite has the property of confining and inducing magnetic flux inside. This property is being considered for use in suppressing leakage magnetic field [5]. Although electromagnetic shielding is possible, leakage magnetic field generated from coils with ferrite have not yet been theorized, so magnetic field analysis and measurement are needed.

The purpose of this paper is to calculate the leakage magnetic field generated from a coil with ferrite for EVs from the theory of air-core coils, and to elucidate the effect of ferrite on the theory. The magnetic fields at 1 m to 20 m from the coil are calculated and evaluated by comparing theoretical and analytical values. This paper is positioned as a basic study for theorizing leakage magnetic field.

2. THEORETICAL CALCULATION OF MAGNETIC FIELD IN AIR-CORE COIL

In this paper, vector potential is used to determine leakage magnetic field generated from the air-core coil. This theory has been used in coil design studies [6]. The vector potential generated at a distance r [m] by the current I [A] flowing in the minute line segment Δs is expressed by Equation (1).

$$\Delta \boldsymbol{A} = \frac{\mu_0 I}{4\pi r} \Delta \boldsymbol{s} \tag{1}$$

Considering a rectangular current loop as shown in Fig. 1 , the vector potential $\boldsymbol{A}$ at any point P(x,y,z) has only A_x and A_y components, as in equations (2) and (3), respectively.

$$A_x \approx \frac{\mu_0 aI}{4\pi r}\left(\frac{1}{r_4} - \frac{1}{r_2}\right) \tag{2}$$

$$A_y \approx \frac{\mu_0 bI}{4\pi r}\left(\frac{1}{r_1} - \frac{1}{r_3}\right) \tag{3}$$

Assuming $a, b \ll r$, the vector potential can be expressed as in equation (4). Hereafter, $r = \sqrt{x^2 + y^2 + z^2}$.

$$\boldsymbol{A}(\boldsymbol{r}) \approx \left(-\frac{\mu_0 abI}{4\pi}\frac{y}{r^3}, \frac{\mu_0 ab}{4\pi}\frac{x}{r^3}, 0\right) \tag{4}$$

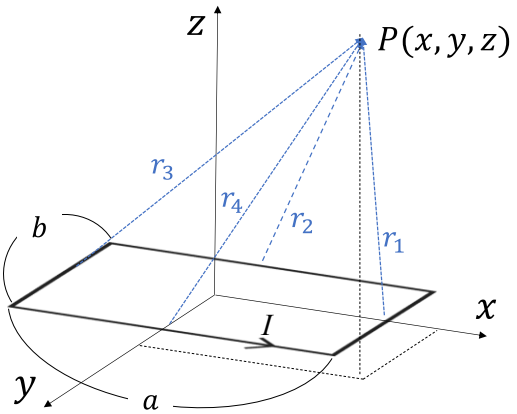

Fig. 1 Current loop of the rectangular model

Calculate the magnetic field at point P using the vector potential expressed in Equation (4). From $B = rotA, B = \mu_0 H$, the magnetic field at point P can be expressed as in equation (5).

$$\boldsymbol{H}(\boldsymbol{r}) = \frac{abI}{4\pi r^5}\begin{pmatrix} 3xz \\ 3yz \\ 2z^2 - x^2 - y^2 \end{pmatrix} \tag{5}$$

If n coils are considered as n current loops as in Fig. 2, ab in equation (5) represents the sum of the areas of each loop. Therefore, ab can be replaced as in equations (6), (7), and (8).

$$ab = \sum_{k=1}^{n} a_k b_k \tag{6}$$

$$a_n = a_1 - 2p(n-1) \tag{7}$$

$$b_n = b_1 - 2p(n-1) \tag{8}$$

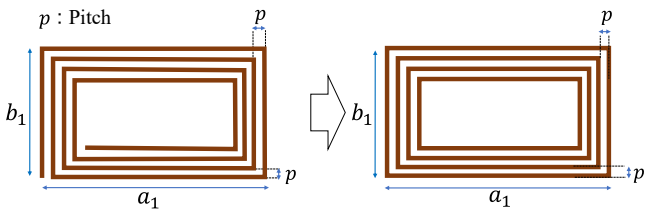

Fig. 2 Substitution of the coil to use for magnetic field calculation.

Next, the magnetic field generated by wireless power transmission is determined. Current loops simulating transmission coil and receiving coil are shown in Fig. 3. The magnetic field $\boldsymbol{H_P}$ at an arbitrary point P is calculated by finding the magnetic field $\boldsymbol{H_{Tx}}$ generated by the primary coil and the magnetic field $\boldsymbol{H_{Rx}}$ generated by secondary coil, respectively, and combining them.

$$|\boldsymbol{H_P}| = |\boldsymbol{H_{Tx}} + \boldsymbol{H_{Rx}}| \tag{9}$$

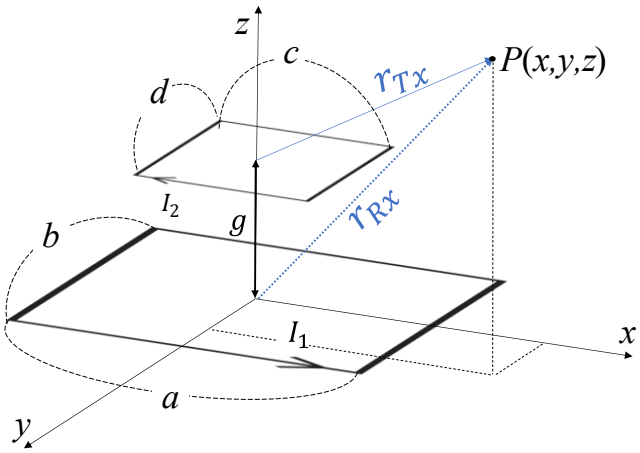

Fig. 3 Position relations of coils used for magnetic field calculation.

When the phase difference between the primary current I_1 [A] and the secondary current I_2 [A] is θ, the magnetic field generated by each coil can be expressed by equations (5)-(10) and (11).

$$\boldsymbol{H_{Tx}} = \begin{matrix} \frac{\sum_{k=1}^{n} a_k b_k}{4\pi}\frac{3xz}{{r_{Tx}}^5}\cdot I_1 \sin\omega t \\ \frac{\sum_{k=1}^{n} a_k b_k}{4\pi}\frac{3yz}{{r_{Tx}}^5}\cdot I_1 \sin\omega t \\ \left(\frac{\sum_{k=1}^{n} a_k b_k}{4\pi}\frac{2z^2 - x^2 - y^2}{{r_{Tx}}^5}\cdot I_1 \sin\omega t\right) \end{matrix} \tag{10}$$

$$\boldsymbol{H_{Rx}} = \begin{matrix} \frac{\sum_{k=1}^{m} c_k d_k}{4\pi}\frac{3x(z-g)}{{r_{Rx}}^5}\cdot I_2 \sin(\omega t + \theta) \\ \frac{\sum_{k=1}^{m} c_k d_k}{4\pi}\frac{3y(z-g)}{{r_{Rx}}^5}\cdot I_2 \sin(\omega t + \theta) \\ \left(\frac{\sum_{k=1}^{m} c_k d_k}{4\pi}\frac{2(z-g)^2 - x^2 - y^2}{{r_{Rx}}^5}\cdot I_2 \sin(\omega t + \theta)\right) \end{matrix} \tag{11}$$

However, $\sum_{k=1}^{n} a_k b_k$ and $\sum_{k=1}^{m} c_k d_k$ are the sum of the current loop areas of the primary and secondary coils, $a_n, b_n \ll r_{Tx}$ and $c_m, d_m \ll r_{Rx}$ respectively. In addition, r_{Tx} [m] and r_{Rx} [m] are the distances from each coil to the point P and are expressed by equations (12) and (13).

$$r_{Tx} = \sqrt{x^2 + y^2 + z^2} \tag{12}$$

$$r_{Rx} = \sqrt{x^2 + y^2 + (z-g)^2} \tag{13}$$

These equations allow us to derive the far field at WPT between air-core coils.

In the next chapter, the magnetic field generated by the coil with ferrite is calculated using the above equations.

3. VERIFICATION BY ELECTROMAGNETIC FIELD ANALYSIS

3.1 ANALYTICAL MODEL

In this paper, a simulation analysis using the MoM method with the electromagnetic field analysis software FEKO is performed and the obtained analytical values are compared with the calculated values. Fig. 4(a) shows an analytical model representing the WPT between two air-core coils, and Fig. 4(b) shows an analytical model representing the WPT when a ferrite core installed only on the power receiving side. The primary coil used in the analysis has an outer diameter of 800 × 600 mm, a pitch of 5.1 mm, and 15 turns, and the secondary coil has an outer diameter of 420 × 420 mm, a pitch of 5.1 mm, and 15 turns. The transmission distance was set to 200 mm, and the resonant frequency of all coils was 85 kHz, which is widely used to feed power to EVs.

The ferrite cores attached to the power receiving coils are PC95 specified in J2954 [1], with a size of 500 × 500 × 5 mm.

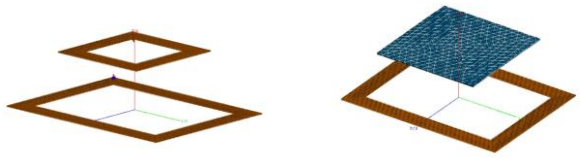

(a) (b)

Fig. 4 Magnetic field analysis model
(a)Transmission and Receiving coils without ferrite core. (b)Transmission coil without ferrite core and receiving coil with ferrite core.

3.2 ANALYTICAL OVERVIEW

The leakage magnetic field generated when a voltage of 842.5 V is applied to the primary coil is analyzed. The magnetic fields in the transverse direction of the car body shown in Fig. 5 and Fig. 6 at distances of 1 to 10 m from the center of the coil, are analyzed, and the obtained analytical values are compared with the values obtained from the equations shown in Chapter 2. The leakage field near the car body is also analyzed, and the analyzed points are shown in Fig. 7. Analytical and calculated values of the magnetic field strength at heights of 0.5 m, 1 m, and 1.5 m at a point 1.08 m away from the center of the coil in the lateral direction of the car body are compared.

In this paper, the current values obtained from the electromagnetic field analysis are used to derive the magnetic field. The peak values and phases of each current obtained are shown in Table 1.

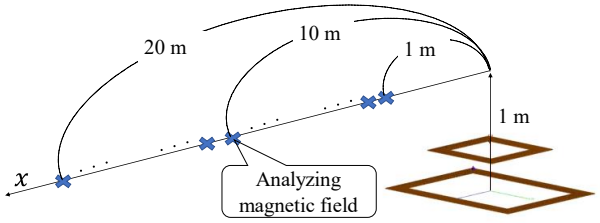

Fig. 5 Magnetic field analysis point of analysis model (a).

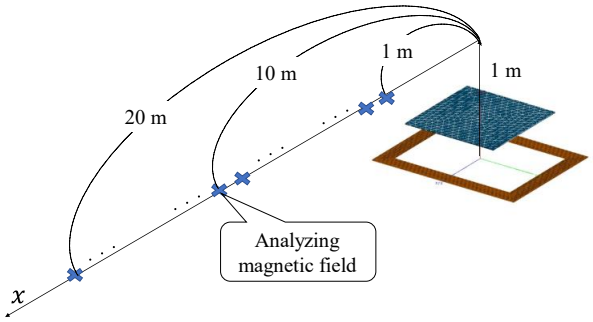

Fig. 6 Magnetic field analysis point of analysis model (b).

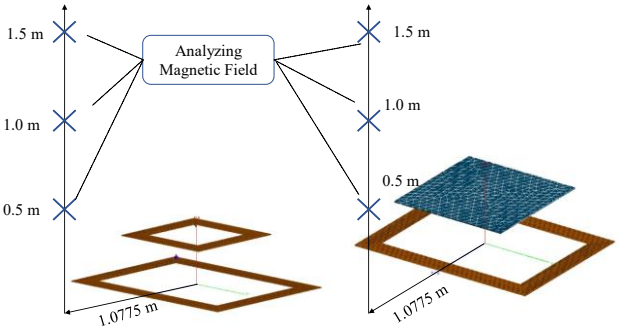

Fig. 7 Magnetic field analysis points in the vicinity of the car body.

Table 1 Current values obtained from magnetic field analysis.

	(a) Non-Ferrite		(b) Ferrite	
	Magnitude [A]	Phase [deg]	Magnitude [A]	Phase [deg]
I_{Tx}	87.3	-0.13	46.5	-4.32
I_{Rx}	51.8	-90.0	38.0	-93.6

3.3 Comparison of analysis results with calculated values

A comparison between the analytical and calculated values is shown in Fig. 8. The difference between the calculated and analytical magnetic fields at 10 m, which is the far end in the EV WPT, is 0.034 dB for the analytical model (a) and 0.086 dB for the analytical model (b). These results correspond to an error of 0.36 % and 0.99 % in the values before conversion to dB values (A/m values), respectively. Table 2 shows a comparison of the magnetic field leakage near the vehicle body at 20 cm from the side (1.08 m from the center of the coil). The maximum error for the air-core coil is 4.87 %, while the maximum error for the coil with ferrite is 4.84 %. The above results confirm that the same theoretical formula can be used to derive the magnetic field as for the air-core coil, even in the case of the ferrite coil.

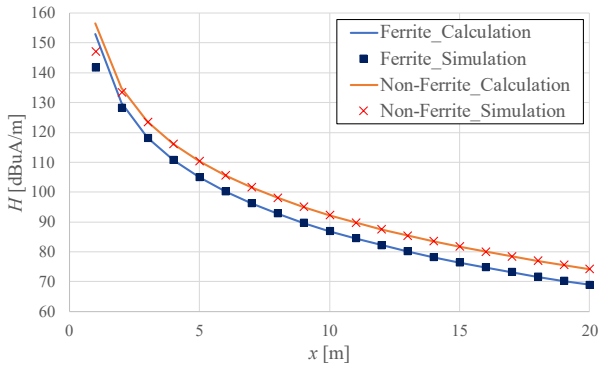

Fig. 8 Comparison of analyzed and calculated values.

Table 2 Comparison of analytical and calculated values in the vicinity of the vehicle body

	(a) Non-Ferrite		(b) Ferrite	
Z [m]	Calculation [μT]	Simulation [μT]	Calculation [μT]	Simulation [μT]
0.5	38.51	37.94	21.07	21.98
1.0	25.54	24.35	14.05	13.52
1.5	14.37	13.73	7.90	7.54

4. CONCLUSION

The theory of air-core coils, based on vector potentials, is used to elucidate the effect of ferrite on the theory of magnetic leakage fields. Comparison with the simulation results shows that at a distance (10 m), the coil with ferrite exhibits an error of 0.99 %, while the air-core coil shows an error of 0.36 %. In the vicinity of the car body, both coils showed an error of less than 5 %. These results show that the theoretical equation for air-core coils can be used to derive magnetic fields even for ferrite-based coils. In this paper, theoretical calculations are performed using only the analytical values for the flowing current. The fact that the derivation is as accurate as that for an air-core coil suggests that the ferrite has little effect on the spread of the magnetic field in the far direction, but it influences the flowing current. If the current flowing in a coil with a ferrite can be derived by desk calculations, it will be possible to estimate the leakage magnetic field generated by numerical calculations only. In the future, it will be a challenge to derive the current values for coils with ferrite cores, as mentioned above. It is necessary to compare the current values obtained from theoretical equations and the results of calculations using phases.

5. References

[1] SAE International, “Wireless Power Transfer for Light-Duty Plug-in/Electric Vehicles and Alignment Methodology J2954," Issued2016-05, Revised 2020-10.

[2] S. Cruciani, T. Campi, F. Maradei and M. Feliziani "Active Shielding Design for Wireless Power Transfer Systems," *in IEEE Transactions on Electromagnetic Compatibility*, vol. 61, no. 6, pp. 1953-1960, Dec. 2019

[3] J. Park, Y. Shin, D. Kim, B. Park and S. Ahn, "Planar Resonance Reactive Shield for Reducing the EMI in Portable WPT Device Application," *2018 IEEE Symposium on Electromagnetic Compatibility, Signal Integrity and Power Integrity (EMC, SI & PI)*, 2018, pp. 419-422.

[4] W. Peng and Z. Chen, "Enhanced Planar Wireless Power Transfer Systems with Ferrite Material," *2018 IEEE Wireless Power Transfer Conference (WPTC)*, 2018, pp. 1-4.

[5] T. Batra, E. Schaltz and S. Ahn, "Reduction of magnetic emission by increasing secondary side capacitor for ferrite geometry based series-series topology for wireless power transfer to vehicles," *2014 16th European Conference on Power Electronics and Applications*, 2014, pp. 1-11.

[6] Y. Yamada, S. Hasegawa, T. Imura and Y. Hori, "Design Method of Coreless Coil Considering Power, Efficiency and Magnetic Field Leakage in Wireless Power Transfer," *the 48th Annual Conference of the IEEE Industrial Electronics Society (IES), IECON2022*, Brussels, Belgium,Oct17-20,2022.